SOME NONSTANDARD DIFFERENTIAL MODELS
WITH APPLICATIONS TO THE POPULATION DYNAMICS
AND COMPUTER VIRUSES PROPAGATION

NIKOLAY KYURKCHIEV[1], VESSELIN KYURKCHIEV[2],
ANTON ILIEV[3], AND ASEN RAHNEV[4]

[1,2,3,4]Faculty of Mathematics and Informatics
University of Plovdiv Paisii Hilendarski
24, Tzar Asen Str., 4000 Plovdiv, BULGARIA

ABSTRACT: In this article we will consider the possibility of approximating the input function $s(t)$ (the nutrient supply for cell growth) of the forms: $s_1(t) = \frac{L-t}{L+t}e^{-mt}$ and $s_2(t) = \frac{(L-t)(P-t)}{(L+t)(P+t)}e^{-mt}$ where L, P and m are parameters. We prove upper and lower estimates for the one–sided Hausdorff approximation of the shifted Heaviside function $h_{t^*}(t)$ by means of the general solutions of the differential equations $y'(t) = ky(t)s_1(t)$ and $y'(t) = ky(t)s_2(t)$ with $y(t_0) = y_0$. We will illustrate the advances of the solution $y(t)$ for approximating and modelling of: "data on the development of the *Drosophila melanogaster* population", published by Raymond Pearl in 1920 (see, also Alpatov, Pearl [21]), *data_Storm_Identifications* (Storm worm was one of the most biggest cyber threats of 2008 [50], [49]), "data on the growth of population of *Oryzaephilus* in renewed wheat" [51], "experimental data for the biomass for thermophilic bacterium *Aeribacillus Pallidus 418*" [52], "experimental data for the tumor spheroid growth" [53], "data for the tumor growth model" [54], "data of attack rates observed on a single link" [55], "data on Intracellular Adenosine Triphosphate (ATP) concentration" [57], "data on HIV/Kaposi's Sarcoma Coinfection Dynamics in Areas of High HIV Prevalence" [58], "data of PI-103 induced concentration-dependent growth inhibition" [59] and "data of Infected Mosquitoes with Dengue" [60].

Numerical examples using *CAS Mathematica*, illustrating our results are given.

1. INTRODUCTION

Sigmoidal functions find multiple applications to population dynamics, analysis of nutrient supply for cell growth in bioreactors, population survival functions, classical predator–prey models, debugging theory and others [23]–[49].

Evidently, the Verhulst model can be considered as a prototype of models used in bioreactor modelling.

In batch growth, the rate of biomass production is given by $\frac{dx}{dt} = \kappa x$, where: $x = $ biomass concentration; $\kappa = $ specific growth rate; $t = $ time.

The rate κ is a function of nutrient supply and therefore can be a function of time (i.e., if nutrient supply is changing with time).

In general, $\kappa = F(S, P, I, X, T, osmotic\ pressure)$; $S = $ substrate concentration; $P = $ product concentration; $I = $ inhibitor concentration.

There, especially in the case of continuous bioreactor, the nutrient supply is considered as an input function $s(t)$ as follows:

$$\frac{dy(t)}{dt} = ky(t)s(t) \tag{1}$$

where s is additional specified.

To the role and choice of nutrient supply for cell growth in bioreactors are devoted to a number of studies [1]–[17].

In [13], the following hyper–logistic equation is considered:

$$\frac{dy(t)}{dt} = ky(t)\frac{2e^{-pt}}{1 + e^{-pt}}$$

$$y(t_0) = y_0,$$

where $k > 0$ and $p > 0$ with general solution:

$$y(t) = y_0 e^{2k(t-t_0) + \frac{2k}{p}\ln(1+e^{pt_0}) - \frac{2k}{p}\ln(1+e^{pt})}.$$

For other approximations of the input function $s(t)$, see, for example [14]–[20]:

$$\begin{cases} \frac{dy(t)}{dt} = ky(t)\frac{1}{(1+t)^p} \\ y(t_0) = y_0; \end{cases}$$

where $p > 0$;

$$\begin{cases} \frac{dy(t)}{dt} = ky(t)\frac{1 + \theta + \theta t}{1 + \theta}e^{-\theta t} \\ y(t_0) = y_0; \end{cases}$$

where $\theta > 0$;

$$\begin{cases} \frac{dy(t)}{dt} = ky(t)\frac{1}{1+mt}e^{-mt} \\ \\ y(t_0) = y_0; \end{cases}$$

where $m > 0$;

$$\begin{cases} \frac{dy(t)}{dt} = ky(t)e^{-\theta(e^{\theta t}-1)} \\ \\ y(t_0) = y_0 \end{cases}$$

where $\theta > 0$;

$$\begin{cases} \frac{dy(t)}{dt} = ky(t)\frac{\theta e^{-\lambda t}}{\theta + (1-\theta)(1-e^{-\lambda t})} \\ \\ y(t_0) = y_0 \end{cases}$$

where $\theta > 0$; $\lambda > 0$;

$$\begin{cases} \frac{dy(t)}{dt} = ky(t)e^{-\theta(e^{\theta t}-1)}(1 - m + me^{-\theta(e^{\theta t}-1)}) \\ \\ y(t_0) = y_0 \end{cases}$$

where $\theta > 0$; $k > 0$ and $0 < m < 1$.

Following the ideas given in [13]–[20], in this paper we consider the following differential models:

$$\begin{cases} \frac{dy(t)}{dt} = ky(t)\frac{L-t}{L+t}e^{-mt} \\ \\ y(t_0) = y_0 \end{cases} \tag{2}$$

$$\begin{cases} \frac{dy(t)}{dt} = ky(t)\frac{(L-t)(P-t)}{(L+t)(P+t)}e^{-mt} \\ \\ y(t_0) = y_0 \end{cases} \tag{3}$$

where L, M and m are parameters.

We prove upper and lower estimates for the one–sided Hausdorff approximation of the shifted Heaviside function $h_{t^*}(t)$ by means of the general solutions of these differential equations.

We will illustrate the advances of the solution $y(t)$ for approximating and modelling of:

- "data on the development of the *Drosophila melanogaster* population", published by biologist Raymond Pearl in 1920 (see, also Alpatov, Pearl [21]);

- *data_Storm_Identifications* [50], [49]);

- "experimental data for the biomass for thermophilic bacterium *Aeribacillus Pallidus 418*" [52];

- "experimental data for the tumor spheroid growth" [53];

- "data for the tumor growth model" [54];

- "data of attack rates observed on a single link" [55];

- "data on the growth of population of *Oryzaephilus* in renewed wheat" [51].

- "data of parasitic growth as a function of the immune serum inhibitory activity" [56];

- "datasets of the Intracellular Adenosine Triphosphate (ATP) concentration" [57];

- "datasets of the number of infected individuals with HIV/Kaposi's Sarcoma with no treatment and with 10% treatment" [58];

- "dataset of PI-103 induced concentration-dependent growth inhibition" [59];

- "dataset of Infected Mosquitoes with Dengue" [60].

2. PRELIMINARIES

Definition 1. The shifted Heaviside step function is defined by

$$
h_{t^*}(t) = \begin{cases} 0, & \text{if} \quad t < t^*, \\ [0,1], & \text{if} \quad t = t^*, \\ 1, & \text{if} \quad t > t^*. \end{cases} \tag{4}
$$

Definition 2. [22] The Hausdorff distance (the H–distance) $\rho(f,g)$ between two interval functions f, g on $\Omega \subseteq \mathbb{R}$, is the distance between their completed graphs $F(f)$ and $F(g)$ considered as closed subsets of $\Omega \times \mathbb{R}$. More precisely,

$$
\rho(f,g) = \max\{ \sup_{A \in F(f)} \inf_{B \in F(g)} ||A - B||, \sup_{B \in F(g)} \inf_{A \in F(f)} ||A - B||\}, \tag{5}
$$

wherein $||.||$ is any norm in $\mathbb{R}^2$, e. g. the maximum norm $||(t, x)|| = \max\{|t|, |x|\}$; hence the distance between the points $A = (t_A, x_A)$, $B = (t_B, x_B)$ in $\mathbb{R}^2$ is $||A - B|| = \max(|t_A - t_B|, |x_A - x_B|)$.
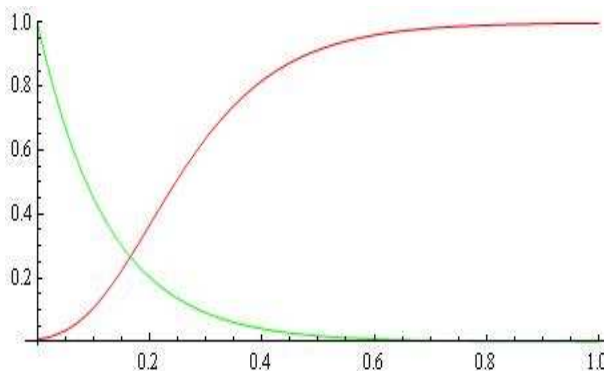
Figure 1: The functions $M(t)$–(red) and $s_1(t)$–(green) for $k = 40; m = 7; L = 2$.

3. MAIN RESULTS.

3.1. THE NEW MODEL (2)

The general solution of the differential equation (2) is of the following form:

$$y(t) = y_0 e^{k\left(\frac{e^{-mt}}{m} + 2e^{Lm}LEi(-m(L+t))\right) - k\left(\frac{e^{-mt_0}}{m} + 2e^{Lm}LEi(-m(L+t_0))\right)}, \qquad (6)$$

where $Ei(.)$ is the exponential integral function defined by

$$Ei(z) = -\int_{-z}^{\infty} \frac{e^{-t}}{t}\, dt$$

(for $z > 0$), where the principal value of the integral is taken.

It is important to study the characteristic - "supersaturation" of the model to the horizontal asymptote.

In this Section we prove upper and lower estimates for the one–sided Hausdorff approximation of the Heaviside step–function $h_{t^*}(t)$ by means of families (6).

Without loss of generality, we consider the following class of this family for:

$$t_0 = 0; \; y_0 = e^{k\left(\frac{1}{m} + 2Le^{Lm}Ei(-Lm)\right)}$$

$$M(t) = e^{k\left(\frac{e^{-mt}}{m} + 2e^{Lm}LEi(-m(L+t))\right)}. \qquad (7)$$

The function $M(t)$ and the "input function" $s(t)$ are visualized on Fig. 1.

Denoting by t^* the unique positive solution of the nonlinear equation:

$$e^{k\left(\frac{e^{-mt^*}}{m} + 2e^{Lm}LEi(-m(L+t^*))\right)} - \frac{1}{2} = 0. \qquad (8)$$

The one–sided Hausdorff distance d between the function $h_{t^*}(t)$ and the sigmoid - (7) satisfies the relation

$$M(t^* + d) = 1 - d. \tag{9}$$

The following theorem gives upper and lower bounds for d

Theorem 1. Let

$$\alpha = -\tfrac{1}{2},$$

$$\beta = 1 + \tfrac{k}{2}\tfrac{L-t^*}{L+t^*}e^{-mt^*} \tag{10}$$

$$\gamma = 2.1\beta.$$

For the one–sided Hausdorff distance d between $h_{t^*}(t)$ and the sigmoid (6) the following inequalities hold for the condition: $\gamma > e^{1.05}$:

$$d_l = \frac{1}{\gamma} < d < \frac{\ln \gamma}{\gamma} = d_r. \tag{11}$$

Proof. Let us examine the function:

$$F(d) = M(t^* + d) - 1 + d. \tag{12}$$

From $F'(d) > 0$ we conclude that function F is increasing.

Consider the function

$$G(d) = \alpha + \beta d. \tag{13}$$

From Taylor expansion we obtain $G(d) - F(d) = O(d^2)$.

Hence $G(d)$ approximates $F(d)$ with $d \to 0$ as $O(d^2)$ (see Fig. 2).

In addition $G'(d) > 0$.

Further, for $\gamma > e^{1.05}$ we have

$$G(d_l) < 0; \quad G(d_r) > 0.$$

This completes the proof of the theorem.

Approximations of the $h_{t^*}(t)$ by model (6) for various k, m and L are visualized on Fig. 3–Fig. 4.

3.2. SOME APPLICATIONS

The proposed model can be successfully used to approximating data from Population Dynamics, Debugging Theory and Theory of Computer Viruses Propagation.
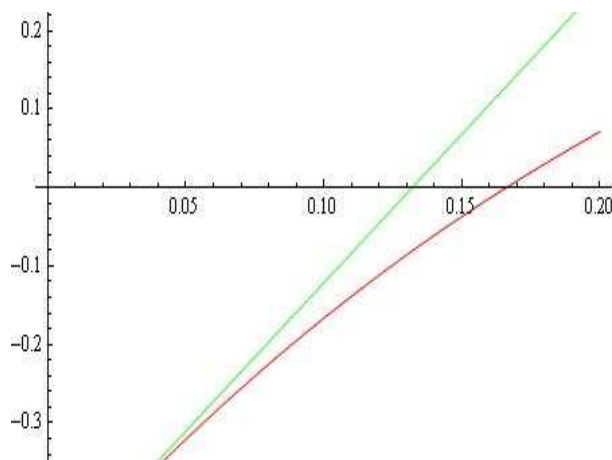
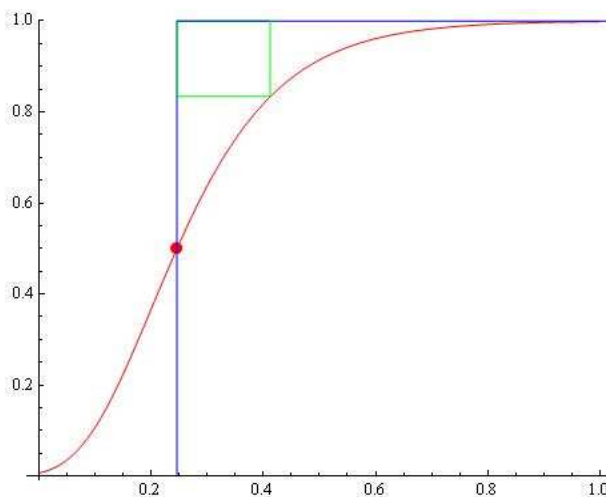Figure 2: The functions $F(d)$ and $G(d)$ for $k = 40$; $m = 7$; $L = 2$.

Figure 3: The model (7) for $k = 40$; $m = 7$; $L = 2$; $t^* = 0.246201$; Hausdorff distance $d = 0.166121$; $d_l = 0.125753$; $d_r = 0.26074$.

3.2.1. APPROXIMATING THE "DATA ON THE DEVELOPMENT OF THE *DROSOPHILA MELANOGASTER* POPULATION"

We will illustrate the advances of the solution $y(t)$ for approximating and modelling of "data on the development of the *Drosophila melanogaster* population", published by biologist Raymond Pearl in 1920 (see, also [21]).
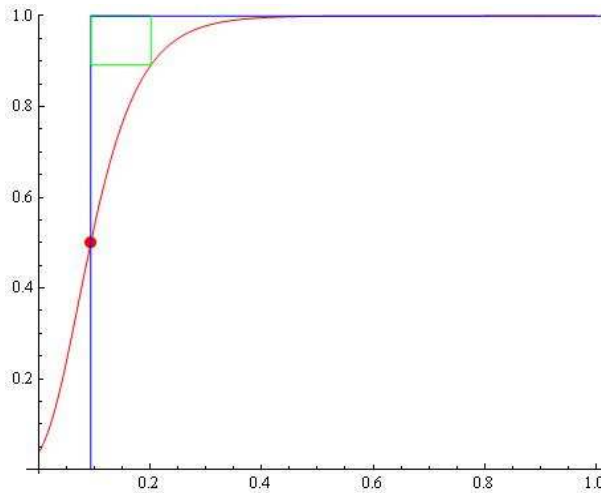
Figure 4: The model (7) for $k = 55$; $m = 16$; $L = 3$; $t^* = 0.0936176$; Hausdorff distance $d = 0.10808$; $d_l = 0.0702664$; $d_r = 0.18650$.

We consider the following data:

$data\_Pearl$

$:= \{\{9, 39\}, \{12, 105\}, \{15, 152\}, \{18, 225\}, \{21, 390\}, \{25, 547\},$

$\{29, 618\}, \{33, 791\}, \{36, 877\}, \{39, 938\}\}.$

After that using the model

$$M^*(t) = \omega e^{k\left(\frac{e^{-mt}}{m} + 2e^{Lm}LEi(-m(L+t))\right)}$$

for $\omega = 2.28719 \times 10^{-7}$, $k = 0.41$, $m = 0.007$ and $L = 42$ we obtain the fitted model (see, Fig. 5).

3.2.2. APPROXIMATING THE
$DATA\_STORM\_IDENTIFICATIONS$ [?], [49]

Storm worm was one of the most biggest cyber threats of 2008. In [50] are noticed particular periods during which their Storm specimen published different IDs every 10 minutes, that behavior cannot account for the very large number of IDs.
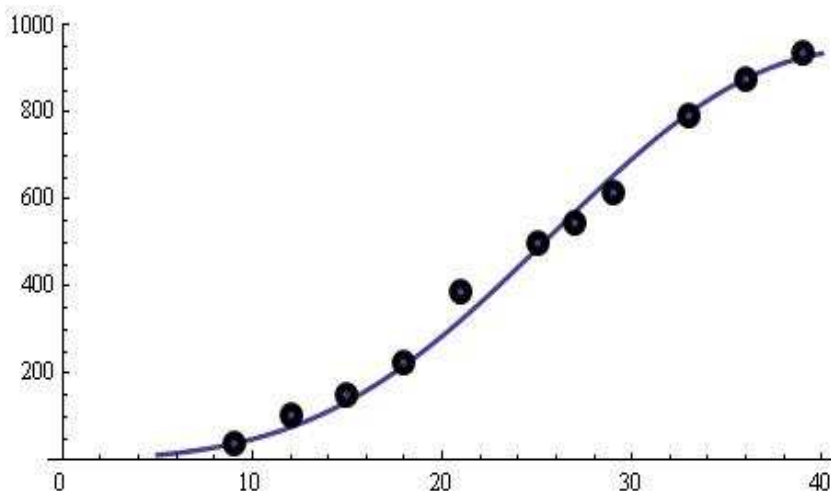
Figure 5: The fitted model $M^*(t)$.

We analyze the following data:

$$data\_Storm\_Identifications :=$$
$$\{\{1, 0.843\}, \{4, 0.926\}, \{5, 0.954\}, \{6, 0.967\}, \{7, 0.976\},$$
$$\{8, 0.981\}, \{9, 0.985\}, \{10, 0.991\}, \{22, 0.995\}, \{38, 0.997\},$$
$$\{51, 0.998\}, \{64, 0.9985\}, \{74, 0.999\}, \{83, 1\}, \{100, 1\}\}.$$

After that using the model $M^*(t)$ for $\omega = 1$, $k = 0.18$, $m = 0.394368$ and $L = 17.1$ we obtain the fitted model (see, Fig. 6).

3.2.3. APPROXIMATING THE DATA: "THE GROWTH OF POPULATION OF *ORYZAEPHILUS* IN RENEWED WHEAT"

We also analyze the following experimental data obtained by the Crombie in 1945 [51]:

$$data\_Crombie\_2$$
$$:= \{\{0, 4\}, \{14, 4\}, \{28, 4\}, \{35, 25\}, \{42, 44\}, \{49, 63\}, \{63, 147\},$$
$$\{77, 285\}, \{91, 345\}, \{105, 361\}, \{119, 405\}, \{133, 471\}, \{147, 420\},$$
$$\{161, 430\}, \{175, 420\}, \{189, 475\}, \{203, 435\}, \{231, 480\}\}.$$

After that using the model $M^*(t)$ for $L = 300$, $k = 2.4$, $m = 0.0505375$ and $\omega = 450$ we obtain the fitted model (see, Fig. 8).

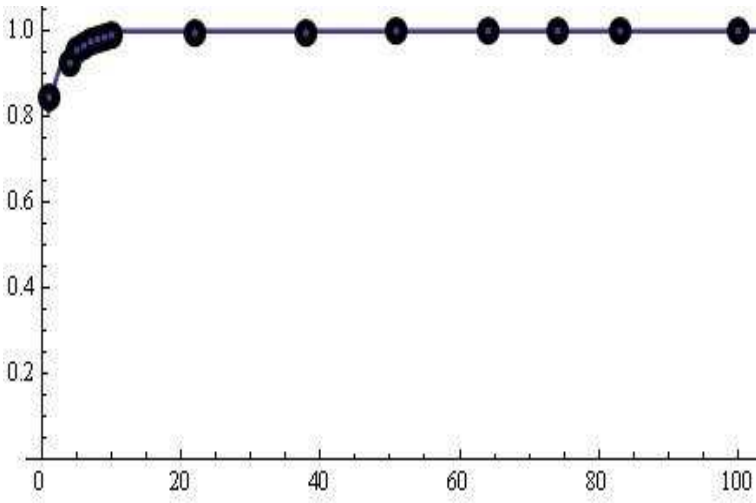The model of Crombie for the *data_Crombie_2* is illustrated in Fig. 7.
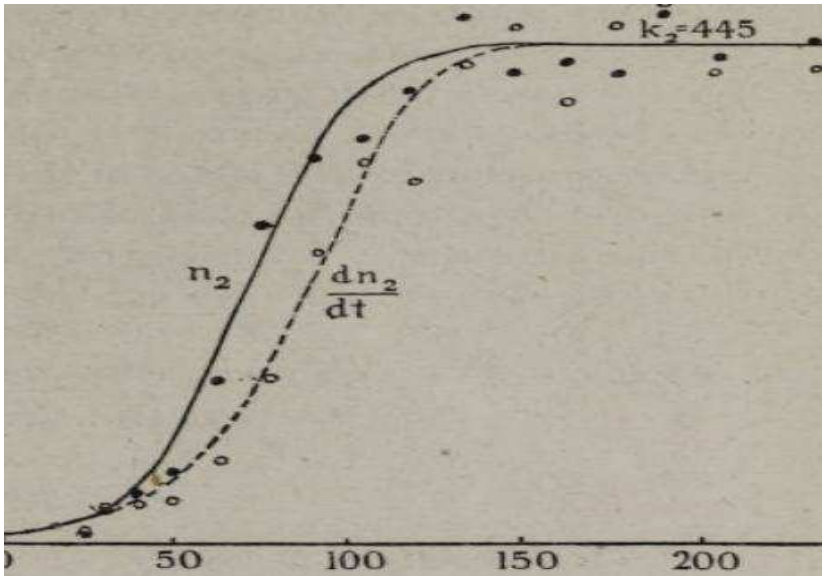
Figure 6: The fitted model $M^*(t)$.

Figure 7: The fitted model by Crombie for the *data_Crombie_2* [51].

3.3. THE NEW MODEL (3)

Without loss of generality, we consider the following class of this family for:

$$t_0 = 0; \; y_0 = e^{\frac{k\left(P - L - 2e^{Lm}Lm(L+P)Ei(-Lm) + 2e^{mP}mP(L+P)Ei(-mP)\right)}{m(L-P)}}$$
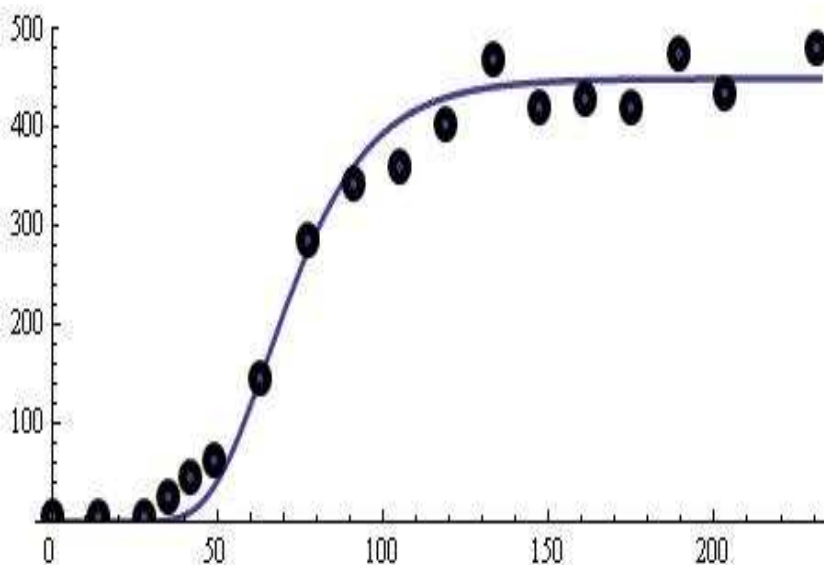
Figure 8: The fitted model $M^*(t)$.

$$M_1(t) = e^{\dfrac{e^{-mt}k\left(P-L-2e^{m(L+t)}Lm(L+P)Ei(-m(L+t))+2e^{m(P+t)}mP(L+P)Ei(-m(P+t))\right)}{m(L-P)}}. \tag{14}$$

It is important to study the characteristic - "supersaturation" of the model to the horizontal asymptote.

The function $M_1(t)$ and the "input function" $s_2(t)$ are visualized on Fig. 9.

Denoting by t^* the unique positive solution of the nonlinear equation $M_1(t^*) - 0.5 = 0$.

The one–sided Hausdorff distance d_1 between the function $h_{t^*}(t)$ and the function - (14) satisfies the relation

$$M_1(t^* + d_1) = 1 - d_1. \tag{15}$$

The estimates for the one–sided Hausdorff approximation of the Heaviside step–function $h_{t^*}(t)$ by means of families (14) can be studied in manner outlined in Theorem 1.

Approximation of the $h_{t^*}(t)$ by model (14) for $k = 3.9$; $m = 5.5$; $L = 50$; $P = 250$ is visualized on Fig. 10.
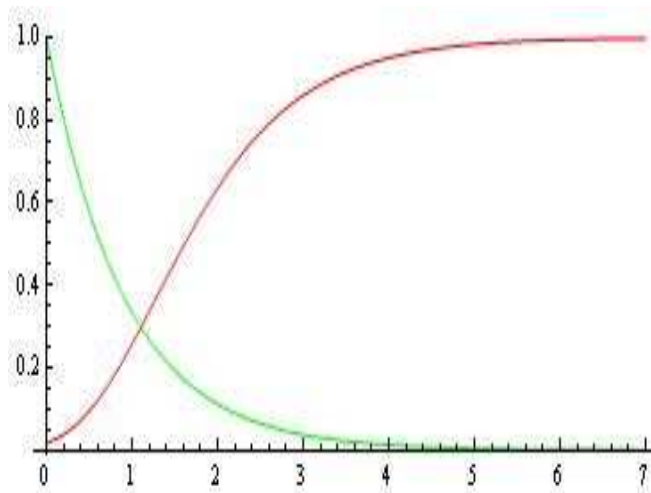
Figure 9: The functions $M_1(t)$–(red) and $s_2(t)$–(green) for $k = 3.9$; $m = 5.5$; $L = 50$; $P = 250$.

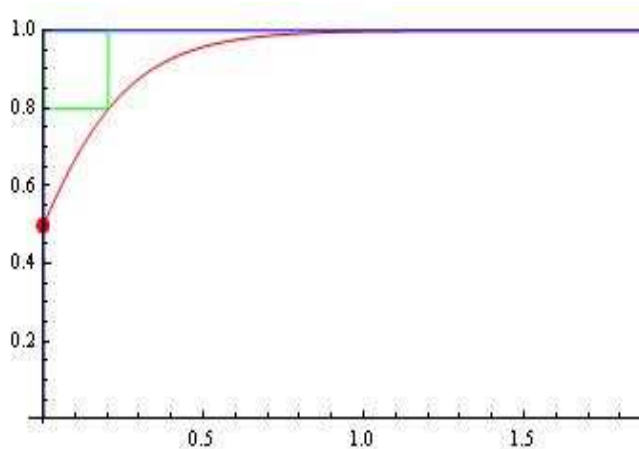Figure 10: The model (14) for $k = 3.9$; $m = 5.5$; $L = 50$; $P = 250$ $t^* = 0.00253276$; Hausdorff distance $d_1 = 0.202142$; $d_{l_1} = 0.162923$; $d_{r_1} = 0.29562$.

3.3.1. APPROXIMATING THE "EXPERIMENTAL DATA FOR THE BIOMASS FOR THERMOPHILIC BACTERIUM *AERIBACILLUS PALLIDUS 418*" [?]

We analyze the following experimental data of the biomass [52]:

$data :=$

$\{\{0, 0\}, \{1, 0\}, \{2, 0\}, \{3, 0\}, \{4, 0\}, \{5, 0.16\}, \{6, 0.45\}, \{7, 1\},$

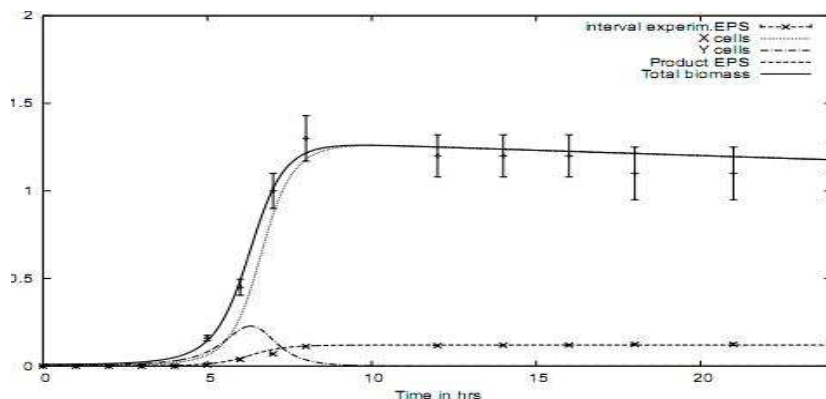$\{8, 1.3\}, \{12, 1.2\}, \{14, 1.2\}, \{16, 1.2\}, \{18, 1.1\}, \{21, 1.1\}, \{24, 1.1\}\}.$
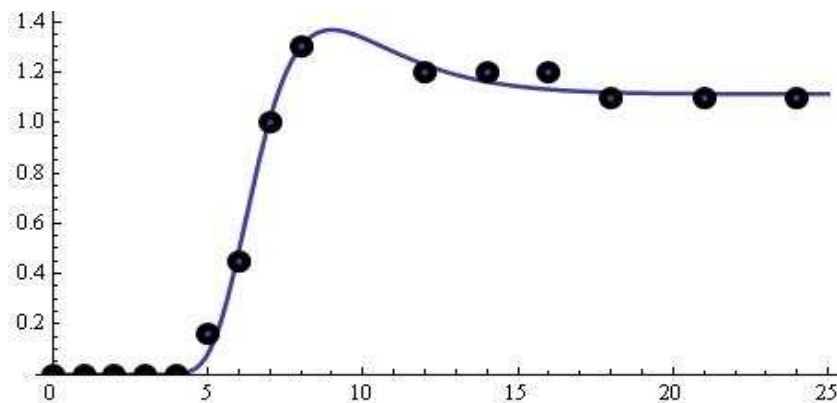
Figure 11: Solution of model [52].

Figure 12: The fitted model $M_1^*(t)$.

After that using the model $M_1^*(t) = \omega M_1(t)$ for $\omega = 1.11385$, $k = 113.818$, $m = 0.42$, $L = 91$ and $P = 25$ we obtain the fitted model (see, Fig. 12).

The solution of model by Radchenkova, Kambourova, Vassilev, R. Alt and Markov is visualized on Fig. 11.

3.3.2. APPROXIMATING THE "EXPERIMENTAL DATA FOR THE TUMOR SPHEROID GROWTH" [?]

Properties of tumor spheroid growth exhibited by a simple mathematical models can be found in [53].

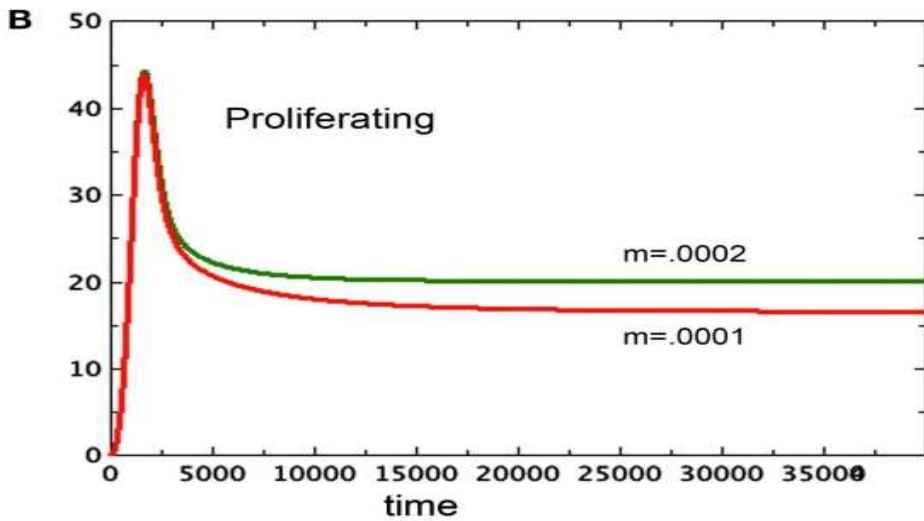Here we analyze the data of the proliferating pool ($m = 0.002$ and $m = 0.001$, see

Figure 13: Solution of model [53].

Fig. 13) [53]:

$data\_m002 :=$

$\{\{0, 0\}, \{385, 5\}, \{577, 10\}, \{769, 15\}, \{833, 20\}, \{1058, 25\},$

$\{1154, 30\}, \{1250, 35\}, \{1346, 40\}, \{2500, 34\}, \{5000, 22\},$

$\{7500, 21\}, \{15000, 20\}, \{35000, 20\}\}.$

$data\_m001 :=$

$\{\{0, 0\}, \{385, 5\}, \{577, 10\}, \{769, 15\}, \{833, 20\}, \{1058, 25\},$

$\{1154, 30\}, \{1250, 35\}, \{1346, 40\}, \{2500, 34\}, \{5000, 21\},$

$\{7500, 19\}, \{15000, 18\}, \{35000, 17\}\}.$

After that using the model $M_1^*(t) = \omega M_1(t)$ for $\omega = 19.6915$, $k = 0.0153181$, $m = 0.0009$, $L = 1650$ and $P = 35000$ we obtain the fitted model (see, Fig. 14).

For $\omega = 18.1353$, $k = 0.0162692$, $m = 0.00088$, $L = 1650$ and $P = 35000$ we obtain the fitted model (see, Fig. 15).
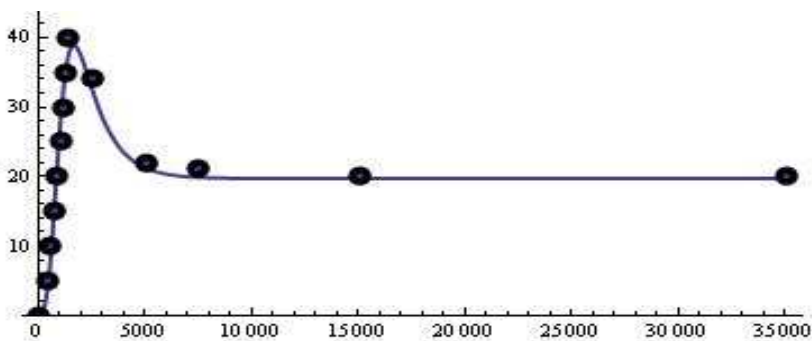
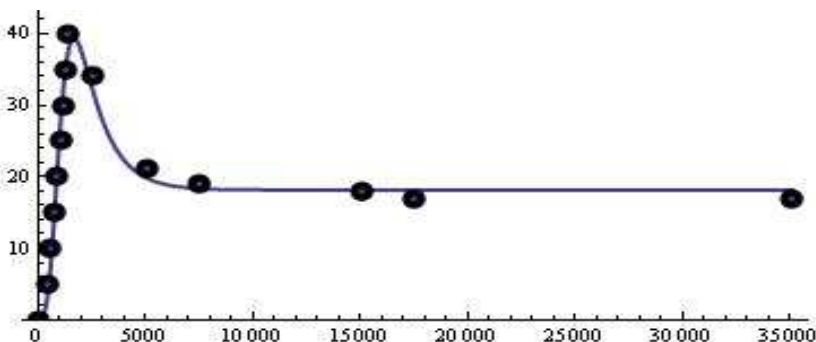Figure 14: The fitted model $M_1^*(t)$ for $m = 0.002$.

Figure 15: The fitted model $M_1^*(t)$ for $m = 0.001$.

3.3.3. APPROXIMATING THE "DATA FOR THE TUMOR GROWTH MODEL" [?]

We analyze the data of the one noise–realization of Proliferating - P (final fit, see Fig. 16) [54]:

$data :=$

$\{\{0, 0\}, \{200, 0.33\}, \{400, 1.16\}, \{600, 1.93\}, \{800, 1.87\}, \{1000, 1.42\},$

$\{1200, 1.35\}, \{1400, 1.02\}, \{1600, 0.90\}, \{1800, 0.83\}, \{2000, 0.95\}\}.$

After that using the model $M_1^*(t) = \omega M_1(t)$ for $\omega = 1.6879$, $k = 0.0403256$, $m = 0.001$, $L = 650$ and $P = 2000$ we obtain the fitted model (see, Fig. 17).
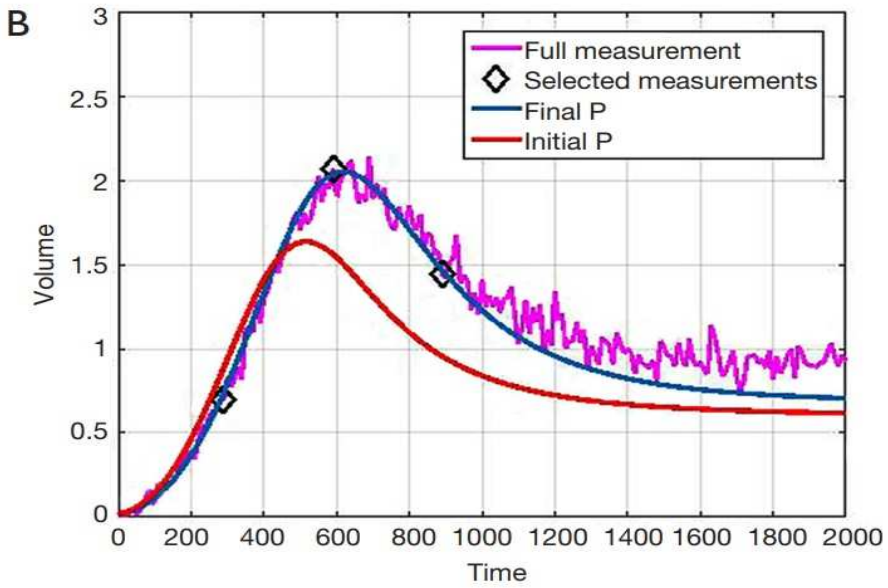
Figure 16: One noise–realization of Proliferating - P (initial and final fit) [54].
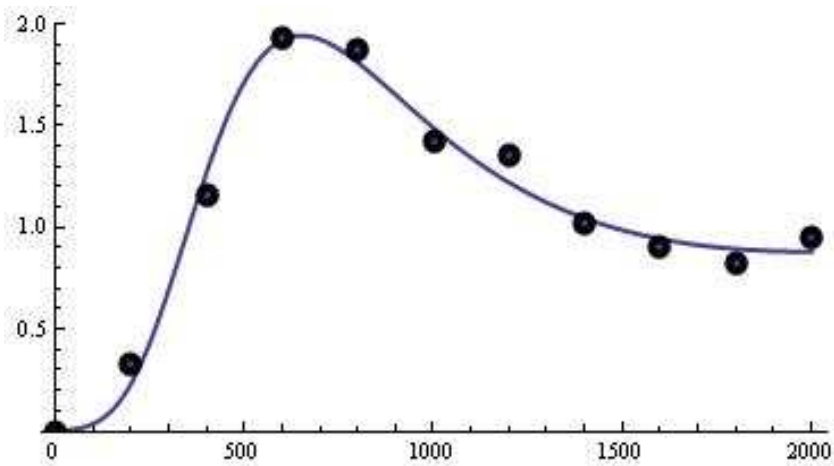

Figure 17: The fitted model $M_1^*(t)$.

3.3.4. APPROXIMATING THE "DATA OF ATTACK RATES OBSERVED ON A SINGLE LINK" [?]

We analyze the data of attack rates observed on a single link, under the hypotheses that links hold (upper curve) or randomly fail (lower curve), see Fig. 18 [55]:

$$data\_upper :=$$

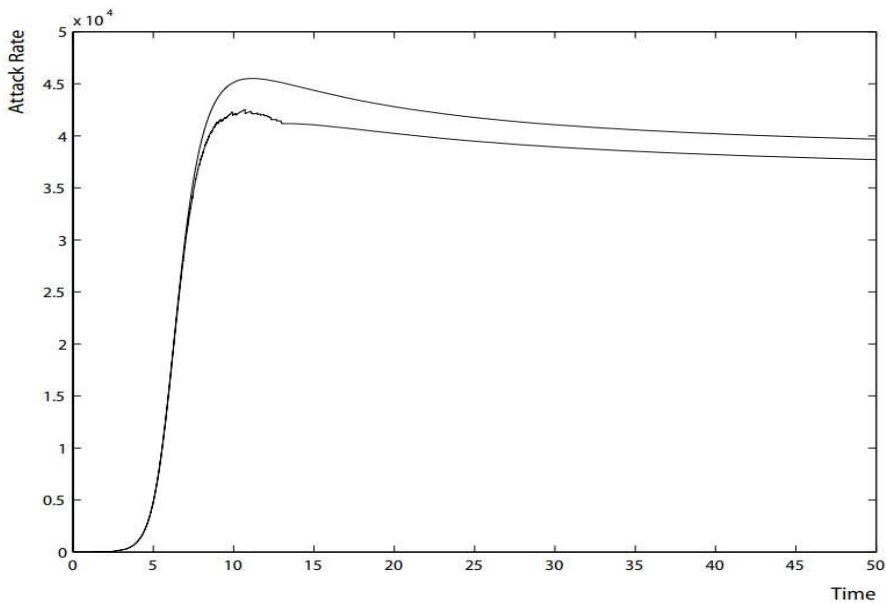$$\{\{0,0\}, \{3,294\}, \{4,1471\}, \{5,10882\}, \{6,35000\}, \{7,63529\},$$

Figure 18: Attack rates observed on a single link [55].

$data\_lower :=$

$\{\{0,0\}, \{3, 294\}, \{4, 1471\}, \{5, 10882\}, \{6, 35000\}, \{7, 63529\},$

$\{8, 78529\}, \{9, 84117\}, \{10, 85294\}, \{11, 85588\}, \{12, 85000\},$

$\{13, 83823\}, \{14, 83529\}, \{15, 83235\}, \{20, 81765\}, \{25, 80294\},$

$\{30, 79118\}, \{35, 78235\}, \{40, 77647\}, \{45, 77059\}, \{50, 76470\}\}.$

After that using the model $M_1^*(t) = \omega M_1(t)$ for $\omega = 83593.2$, $k = 43.0354$, $m = 0.42$, $L = 10.2$ and $P = 150$ we obtain the fitted model (see, Fig. 19).

For $\omega = 79727.2$, $k = 37.3208$, $m = 0.42$, $L = 10.5$ and $P = 95$ we obtain the fitted model (see, Fig. 20).

As should expected, the experiments conducted (see, Sections 3.2 - 3.3) show a very good approximation of data from the field of population dynamics and computer viruses propagation, with suggested in this article, modified logistic model.

Remark. Parasitic infections are often chronic and affect many people.

The effect of antibody on malaria parasites as well as the differential model of parasitic growth as a function of the immune serum inhibitory activity are well studied (see, e.g. [56]).
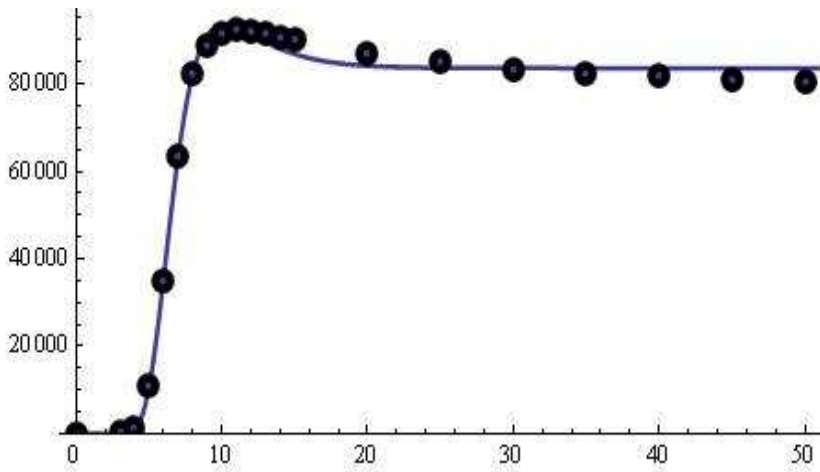
Figure 19: The fitted model $M_1^*(t)$.
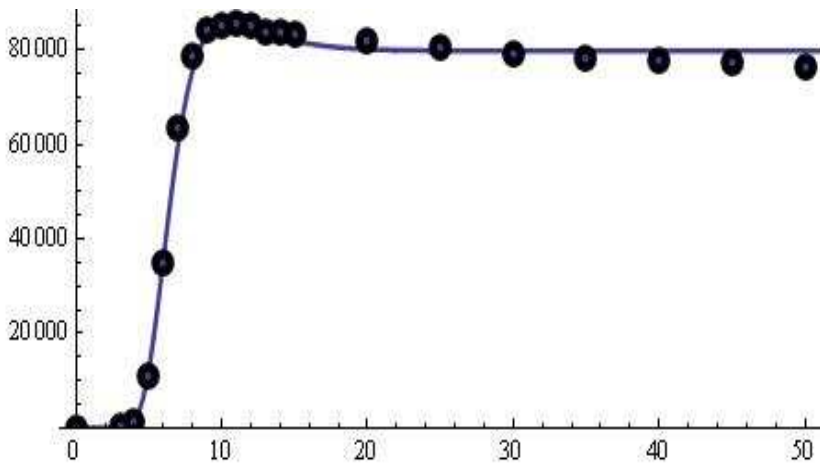
Figure 20: The fitted model $M_1^*(t)$.

The presence of immune serum blocks the continued increase in number of Plasmodium Knowlesi (a malaria parasite of monkeys), see Fig. 21: Parasite growth and immune serum (blue) [56].
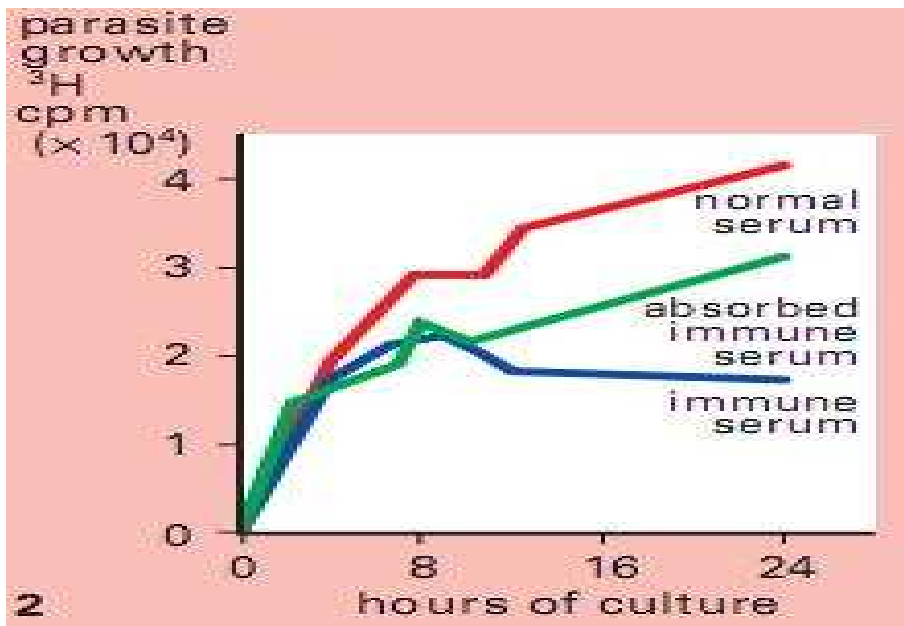
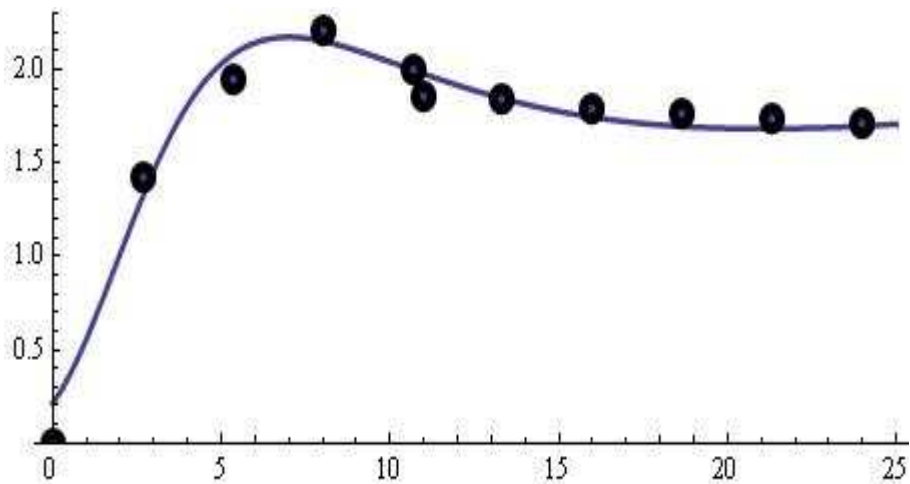Figure 21: Parasitic growth as a function of the immune serum inhibitory activity (blue) [56].

Figure 22: The fitted model $M_1^*(t)$.

We analyze the following data:

$$data\_immune\_serum :=$$

$$\{\{0, 0\}, \{2.67, 1.42\}, \{5.33, 1.95\}, \{8, 2.21\}, \{10.67, 2\}, \{11, 1.86\},$$

$$\{13.33, 1.84\}, \{16, 1.79\}, \{18.67, 1.78\}, \{21.33, 1.74\},$$

$$\{24, 1.7192059\}\}.$$

After that using the model $M_1^*(t) = \omega M_1(t)$ for $\omega = 2.21098$, $k = 1.21016$, $m = 0.088$, $L = 7$ and $P = 21.03$ we obtain the fitted model (see, Fig. 22).

4. APPROXIMATING THE ATP CONCENTRATION

The Intracellular Adenosine Triphosphate (ATP) concentration (see, Fig. 23) [57] indicates that the stationary state (ss) is asymptotically stable for both cell types, assuming the initial concentration of glucose extracellular (Glu_{out}) as a control parameter.

We analyze the following datasets [57]:

$$data\_A := \{\{0, 0.7\}, \{0.2, 9.85\}, \{0.3, 9.9\}, \{0.4, 9.85\}, \{0.6, 9.5\},$$

$$\{0.8, 9.2\}, \{1, 8.95\}, \{1.2, 8.75\}, \{1.4, 8.65\}, \{1.6, 8.55\}, \{1.8, 8.5\},$$

$$\{2, 8.47\}, \{2.2, 8.45\}, \{2.4, 8.44\}, \{3, 8.42\}, \{4, 8.4\}, \{5, 8.37\}\};$$

$$data\_B := \{\{0, 7.9\}, \{0.05, 8.55\}, \{0.2, 7.6\}, \{0.4, 7.25\}, \{0.6, 7.15\},$$

$$\{0.8, 7.25\}, \{1, 7.3\}, \{1.2, 7.4\}, \{1.4, 7.5\}, \{1.6, 7.55\}, \{1.8, 7.62\},$$

$$\{2, 7.65\}, \{2.2, 7.67\}, \{2.4, 7.69\}, \{2.6, 7.71\}, \{2.8, 7.72\}, \{3, 7.73\},$$

$$\{4, 7.73\}, \{5, 7.73\}\};$$

$$data\_C := \{\{0, 5.2\}, \{1, 9.7\}, \{2, 9.6\}, \{4, 9.4\}, \{6, 9.2\}, \{8, 8.9\},$$

$$\{10, 8.7\}, \{12, 8.5\}, \{14, 8.3\}, \{16, 8.2\}, \{18, 8.1\}, \{20, 8\}, \{22, 7.9\},$$

$$\{24, 7.87\}, \{26, 7.84\}, \{30, 7.82\}, \{40, 7.8\}, \{50, 7.8\}\};$$

$$data\_D := \{\{0, 5.4\}, \{1, 10.5\}, \{2, 10.3\}, \{4, 9.3\}, \{6, 5.8\}, \{8, 4.2\},$$

$$\{10, 4\}, \{12, 3.8\}, \{20, 3.8\}, \{30, 3.8\}, \{40, 3.8\}, \{50, 3.8\}\}.$$

The fitted models (see, Fig. 24):
A) $M_1^*(t)$ - $L = 0.3$; $P = 100$; $m = 6$; $\omega = 8.58611$; $k = 34.841$;
B) $M_1^*(t)$ - $L = 0.79$; $P = 4$; $m = 0.492$; $\omega = 7.58418$; $k = -0.515663$;
C) $M_1^*(t)$ - $L = 2.9$; $P = 3500$; $m = 0.2$; $\omega = 7.63379$; $k = 0.242045$;
D) $M_1^*(t)$ - $L = 1.75$; $P = 50$; $m = 0.23$; $\omega = 3.48735$; $k = 1.20129$.
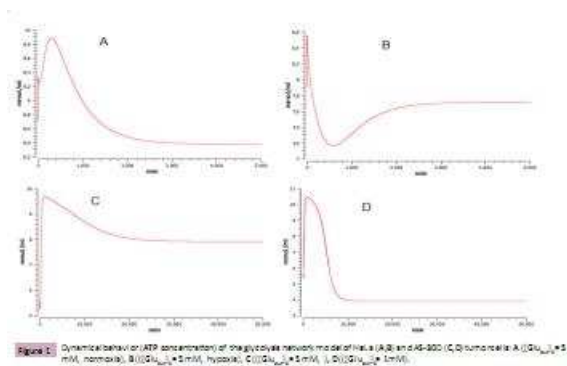
Figure 23: [57]

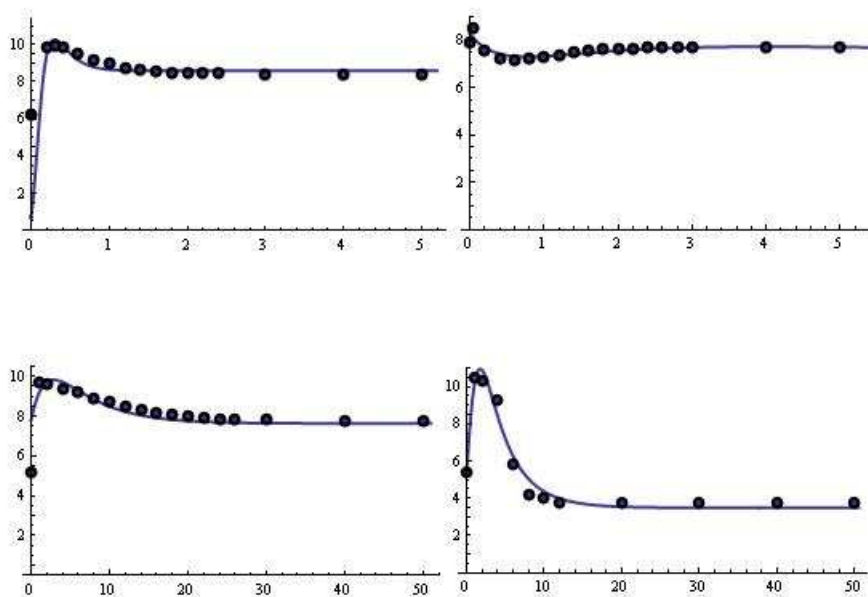Figure 24: The fitted models $M_1^*(t)$.

5. APPROXIMATING THE HIV/KAPOSI'S SARCOMA COINFECTION DYNAMICS

The model for HIV/Kaposi's Sarcoma Coinfection Dynamics in Areas of High HIV Prevalence is presented in [58].

Here we will fit the number of infected individuals with HIV/Kaposi's Sarcoma with no treatment (see Fig. 25) and with 10% treatment (see Fig. 27).
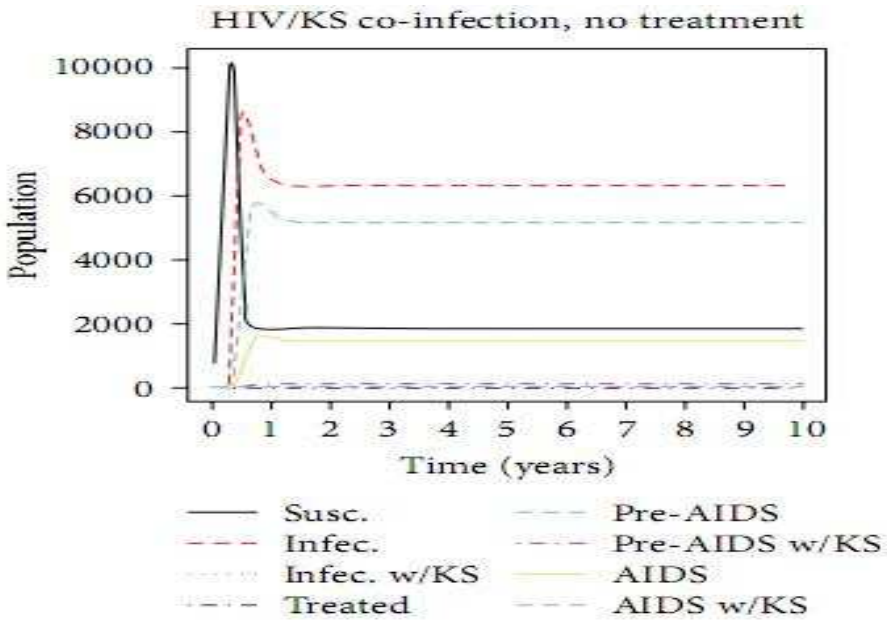
Figure 25: [58].

We analyze the given datasets [58]:

$data\_HIV/KS\_co-infection\_no\_treatment := \{\{0.24138, 0\},$

$\{0.31034, 2000\}, \{0.37931, 4000\}, \{0.44828, 6000\}, \{0.48276, 8000\},$

$\{0.49655, 8480\}, \{0.51724, 8590\}, \{0.55172, 8440\}, \{0.86207, 6670\},$

$\{1, 6440\}, \{1.17241, 6300\}, \{1.34483, 6260\}, \{2, 6220\}, \{6, 6220\},$

$\{7, 6190\}, \{10, 6190\}\};$

$data\_HIV/KS\_co-infection\_10\%\_treatment := \{\{0.27586, 0\},$

$\{0.44828, 5680\}, \{0.51724, 5840\}, \{0.55172, 5600\}, \{0.79310, 3640\},$

$\{1, 3440\}, \{1.20690, 3360\}, \{2, 3360\}, \{10, 3360\}\}.$

The fitted models (see, Fig. 26 and Fig. 28):
A) $M_1^*(t)$ - $L = 0.58$ $P = 10$; $m = 5.53$; $\omega = 6121.15$; $k = 449.493$;
C) $M_1^*(t)$ - $L = 0.5$; $P = 10$; $m = 9.35$; $\omega = 3355.32$; $k = 7590.8$;

Since the mathematical model of HIV/Kaposi's Sarcoma Coinfection Dynamics in Areas of High HIV Prevalence is well-studied, we will note that it is described with a known system of stratified differential equations which we will not explore here.

Figure 26: The fitted model $M_1^*(t)$.
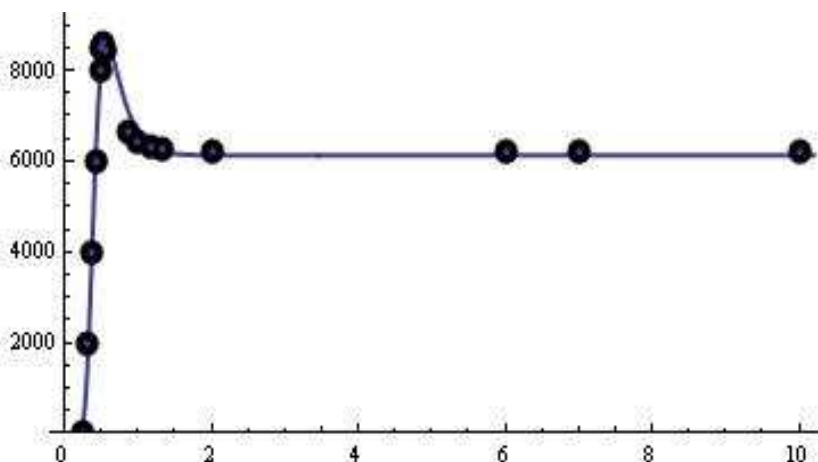
Without be a specialists on this subject we will only note that the approximation of the above-mentioned data for "infected individuals" - Fig. 25 (red-dashed) and Fig. 27 (red-dashed) with the model function discussed in this chapter gives us unexpected good results for which we have insufficient scientific reasoning at this stage.

The specialists working in the field of "reaction-kinetic mechanisms" have the word.

6. APPROXIMATING TUMOR SPHEROID GROWTH INHIBITION WITH PI-103

For evaluation of the effects of molecularly targeted agents on three-dimensional tumor growth kinetics, 4-day-old spheroids (for example, U-87 MG) were treated with compounds for 72 h [59]. The results are visualized by logarithmic scale of 'X' axis. PI-103 induced concentration-dependent growth inhibition.

We analyze the following dataset [59]:

$$data\_PI - 103\_induced\_concetr. - depen.\_growth\_inhibition :=$$

$$\{\{0.009, 94.554\}, \{0.017, 93.564\}, \{0.053, 86.634\},$$

$$\{0.080, 76.733\}, \{0.180, 58.911\}, \{0.450, 35\},$$

$$\{0.721, 20\}, \{0.984, 15\}, \{2, 14\}, \{3.628, 12\}\}.$$

By the help of the model $M_1^*(t) = \omega M_1(t)$ for $L = 1.9$; $P = 3.2$; $m = 0.1$; $\omega = 0.000728774$ and $k = -3.79042$ we obtain the fitted model (see, Fig. 29).
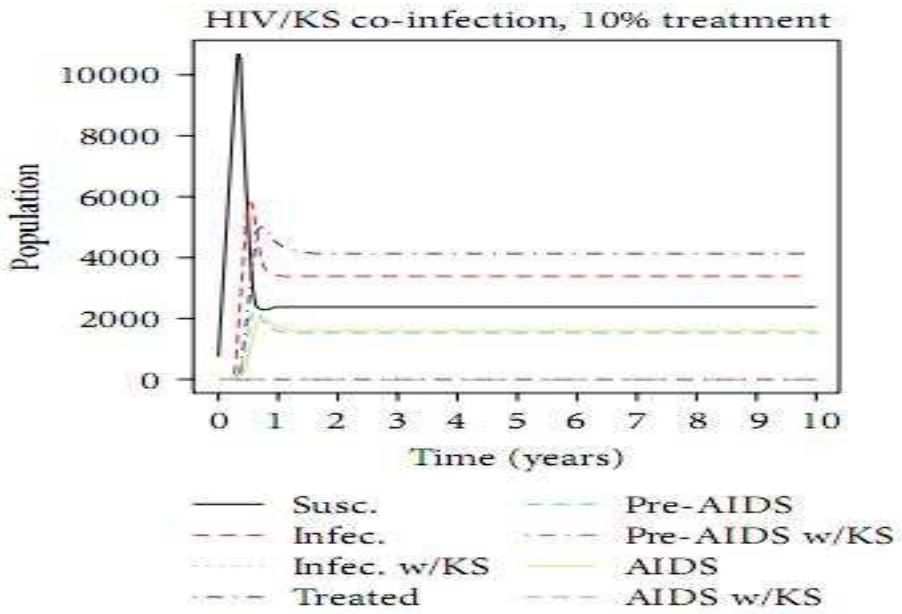
Figure 27: [58].

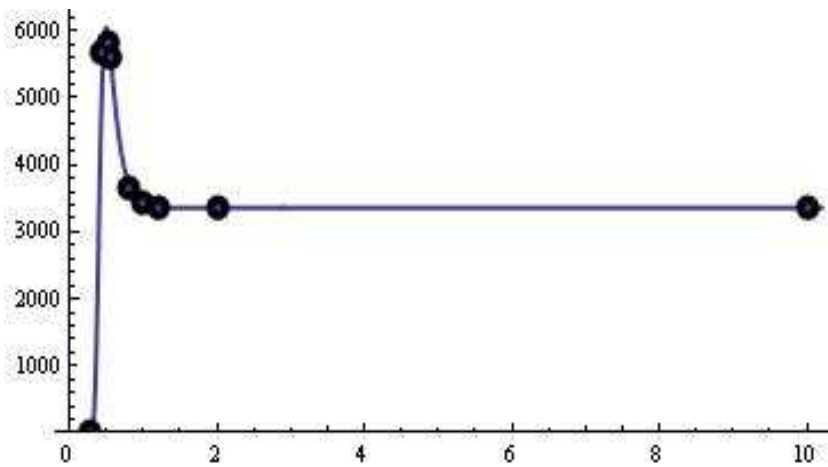
Figure 28: The fitted model $M_1^*(t)$.

7. APPROXIMATING INFECTED MOSQUITOES WITH DENGUE

In Fig. 30 [60] (red line), there is no considerable difference between the cases of without control and with control in the dengue-infected mosquitoes.
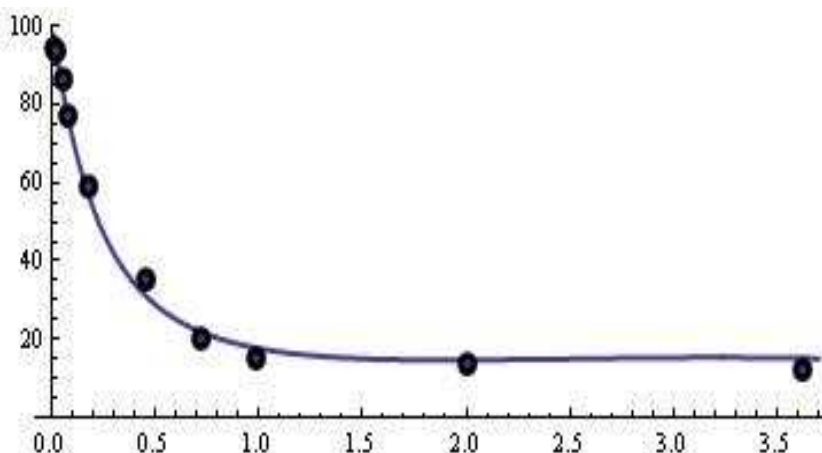
Figure 29: The fitted model $M_1^*(t)$.

We will use the following dataset which we took from Fig. 30 [60] (red line):

$$data\_Infected\_Mosquitoes\_with\_Dengue := \{\{0, 111\},$$

$$\{0.455, 200\}, \{1.364, 300\}, \{2.045, 400\}, \{3.182, 500\},$$

$$\{4.545, 600\}, \{5, 630\}, \{6.818, 700\}, \{7.5, 730\}, \{10, 778\},$$

$$\{12.5, 787\}, \{15, 776\}, \{17.5, 750\}, \{20, 713\}, \{21.136, 700\},$$

$$\{26.591, 600\}, \{30, 539\}, \{32.272, 500\}, \{38.409, 400\},$$

$$\{40, 374\}, \{46.136, 300\}, \{50, 259\}, \{56.591, 200\},$$

$$\{60, 167\}, \{65, 139\}, \{70, 113\}, \{72.727, 100\}, \{80, 64\},$$

$$\{85, 45\}, \{90, 25\}, \{95, 15\}, \{100, 0\}\}.$$

By the usage of the model $M_1^*(t) = \omega M_1(t)$ for $\omega = 10.3733$; $k = 0.208036$; $m = 0.185$; $L = 14.45$ and $P = 4590$ we receive the fitted model (see, Fig. 31).

8. CONCLUSION.

A special choice of nutrient supply for cell growth in a continuous bioreactor is introduced.

We prove upper and lower estimates for the one–sided Hausdorff approximation of the shifted Heaviside function $h_{t^*}(t)$ by means of the general solutions of the dif-
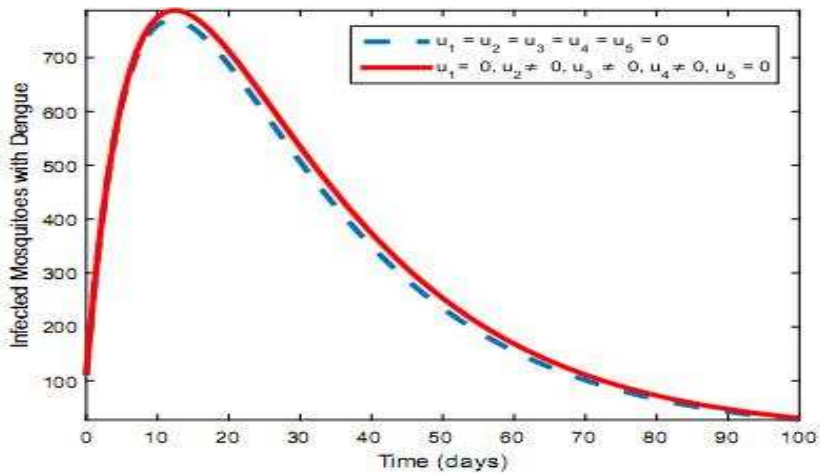
Figure 30: [60].
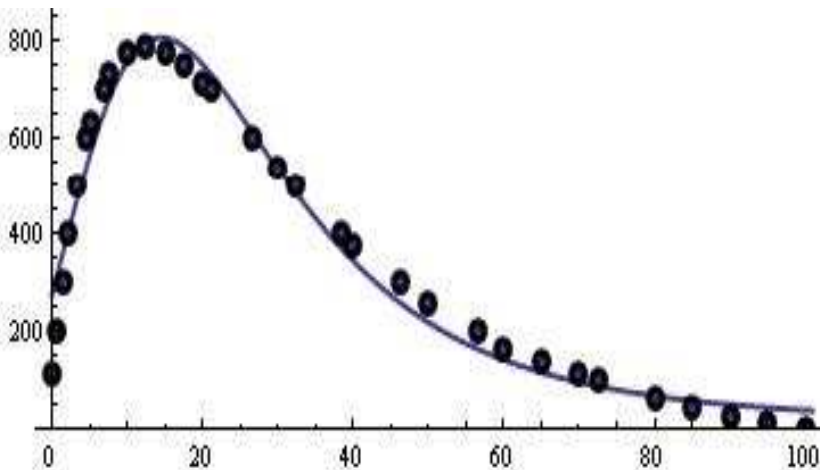
Figure 31: The fitted model $M_1^*(t)$.

ferential equations:$y'(t) = ky(t)s_1(t)$ and $y'(t) = ky(t)s_2(t)$ with $y(t_0) = y_0$, where $s_1(t) = \frac{L-t}{L+t}e^{-mt}$ and $s_2(t) = \frac{(L-t)(P-t)}{(L+t)(P+t)}e^{-mt}$.

Since the determination of the inflexion points of the functions $S_1(t)$ and $S_2(t)$ is not a difficult, we will note that the parameters L and P can be used as "limiters of specifically located data".

We propose a software module within the programming environment *CAS Mathematica* for the analysis of the considered family of functions.

The module offers the following possibilities:

- calculation of the H-distance between the h_{t*} and the model $M(t)$ (6);

- generation of the functions under user defined values of the parameters k, m and L;

- generation of the functions by model (14) under user defined values of the parameters k, m, L and P;

- numerical solution of the differential models (2) and (3) and opportunities for comparison with other logistics models;

- software tools for animation and visualization.

There are many approaches for modelling computer viruses propagation.

Here we give new modelling ways and make subsequent steps to give more precise approximations of these epidemics.

At present, the authors are working hard to construct and study new differential models designed to approximate "specific" data from the propagation of computer viruses usually concentrated in unexpected intervals.

Such results will help to fully capturing the epidemic outbreak of virus spreading.

We can conclude that the Hausdorff apparatus used to evaluate "supersaturation" in the treatment of relational problems in various scientific fields is proved its sufficiently reliable. For other applications of Hausdorff distance, see [61].

ACKNOWLEDGMENTS

REFERENCES

[1] P. Pathi, T. Ma, R. Locke, Role of nutrient supply on cell growth in bioreactor design for tissue engineering of hematopoietic cells, *Biotechnology and Bioengineering*, **89**, No. 7 (2005).

[2] N. Li, H. Y. Sun, Q. L. Zhang, The dynamics and bifurcation control of a singular biological economic model, *Int. J. of Automat. and Comp.*, **9**, No. 1 (2012), 1–7.

[3] T. Egli, M. Zinn, The concept of multiple–nutrient–limited growth of microorganisms and its application in biotechnological processes, *Biotechnol. Adv.*, **22** (2003), 5–43.

[4] D. F. Gerson, M. M. Kole, B. Ozum, M. N. Oguztoreli, Substrate concentration control in bioreactors, *Biotechnology and Genetic Engineering Reviews,* **6**, No. 1, 1988, 67–150.

[5] Y. Zhang, Q. L. Zhang, L. C. Zhao, Analysis and feedback control for a class of bioeconomic systems, *J. Control Eng. of China*, **14**, No. 6 (2007), 599–603.

[6] Y. Zhang, Q. L. Zhang, L. C. Zhao, Bifurcations and control in singular biological economic model with stage structure, *J. of Syst. Eng.*, **22**, No. 3 (2007), 233–238.

[7] S. Luan, B. Liu, L. X. Zhang, Dynamics on a single-species model in a polluted environment, *J. of Biomath.*, **26**, No. 4 (2011), 689–694.

[8] V. Noris, E. Maurice, D. Maurice, Modelling Biological Systems with Competitive Coherence, *J. of Appl. Math.*, (2012), 1–20.

[9] M. Borisov, N. Dimitrova, V. Beshkov, Stability analysis of a bioreactor model for biodegradation of xenobiotics, *Comp. and Math. with Appl.,* **64**, (2012).

[10] N. Dimitrova, Local bifurcations in a nonlinear model of a bioreactor, *Serdica J. Computing*, **3** (2009), 107–132.

[11] T. Ivanov, N. Dimitrova, Analysis of a Bioreactor Model with Microbial Growth Phases and Spatial Dispersal, *Biomath Communications*, **2**, No. 2 (2016).

[12] N. Kyurkchiev, S. Markov, G. Velikova, The dynamics and control on a singular bio-economic model with stage structure, *Biomath Communications*, **2**, No. 2 (2015).

[13] N. Kyurkchiev, Investigations on a hyper-logistic model. Some applications, *Dynamic Systems and Applications*, **28**, No. 2 (2019), 351–369.

[14] E. Angelova, A. Golev, T. Terzieva, O. Rahneva, A study on a hyper–power–logistic model. Some applications, *Neural, Parallel and Scientific Computations*, **27**, No. 1 (2019), 45–57.

[15] N. Kyurkchiev, A. Iliev, A. Rahnev, On a special choice of nutrient supply for cell growth in a continuous bioreactor. Some modeling and approximation aspects, *Dynamic Systems and Applications*, **28**, No. 3 (2019), 587–606.

[16] N. Kyurkchiev, S. Markov, On a logistic differential model. Some applications, *Biomath Communications*, **6**, No. 1 (2019), 34–50.

[17] N. Kyurkchiev, A. Iliev, A. Rahnev, A special choice of nutrient supply for cell growth in logistic differential model. Some applications, *Proc. of the NTADES Series of AIP*, (2019). (to appear)

[18] N. Kyurkchiev, A. Iliev, A. Golev, A. Rahnev, On a special choice of nutrient supply with Marshall–Olkin correction. Some applications, *Communications in Applied Analysis*, **23**, No. 3 (2019), 401–419.

[19] E. Angelova, A. Malinova, V. Kyurkchiev, O. Rahneva, Investigations on a Logistic Model with Weighted Exponential Gompertz Type Correction. Some Applications,*Neural, Parallel, and Scientific Computations*, **27**, No. 2 (2019), 105–114.

[20] E. Angelova, T. Terzieva, V. Kyurkchiev, O. Rahneva, On a logistic differential model, *Neural, Parallel, and Scientific Computations*, **27**, No. 2 (2019), 93–104.

[21] W. Alpatov, R. Pearl, Experimental studies on the duration of life. XII. Influence of temperature during the larval period and adult life on the duration of the life of the imago of Drosophila melanogaster, *Am. Nat.*, **69**, No. 63 (1929), 37–67.

[22] F. Hausdorff, *Set Theory*, 2nd ed., Chelsea Publ., New York (1962).

[23] N. Kyurkchiev, S. Markov, On the Hausdorff distance between the Heaviside step function and Verhulst logistic function, *J. Math. Chem.*, **54**, No. 1 (2016), 109–119.

[24] N. Kyurkchiev, S. Markov, *Sigmoid functions: Some Approximation and Modelling Aspects*, LAP LAMBERT Academic Publishing, Saarbrucken (2015), ISBN 978-3-659-76045-7.

[25] N. Kyurkchiev, A. Iliev, S. Markov, *Some techniques for recurrence generating of activation functions*, LAP LAMBERT Academic Publishing (2017), ISBN: 978-3-330-33143-3.

[26] R. Anguelov, N. Kyurkchiev, S. Markov, Some properties of the Blumberg's hyper-log-logistic curve, *Biomath*, **7**, No. 1 (2018), 8 pp.

[27] A. Iliev, N. Kyurkchiev, S. Markov, On the Approximation of the step function by some sigmoid functions, *Mathematics and Computers in Simulation*, **133** (2017), 223–234.

[28] A. Iliev, N. Kyurkchiev, S. Markov, Approximation of the cut function by Stannard and Richards sigmoid functions, *IJPAM*, **109**, No. 1 (2016), 119–128.

[29] S. Markov, A. Iliev, A. Rahnev, N. Kyurkchiev, A note on the Log-logistic and transmuted Log-logistic models. Some applications, *Dynamic Systems and Applications*, **27**, No. 3 (2018), 593–607.

[30] S. Markov, N. Kyurkchiev, A. Iliev, A. Rahnev, On the approximation of the cut functions by hyper-log-logistic function, *Neural, Parallel and Scientific Computations*, **26**, No. 2 (2018), 169–182.

[31] N. Kyurkchiev, A Note on the Volmer's Activation (VA) Function, *C. R. Acad. Bulg. Sci.*, **70**, No. 6 (2017), 769–776.

[32] N. Kyurkchiev, A note on the new geometric representation for the parameters in the fibril elongation process. *C. R. Acad. Bulg. Sci.*, **69**, No. 8 (2016), 963–972.

[33] N. Kyurkchiev, S. Markov, On the numerical solution of the general kinetic "K-angle" reaction system, *Journal of Mathematical Chemistry*, **54**, No. 3 (2016), 792–805.

[34] N. Guliyev, V. Ismailov, A single hidden layer feedforward network with only one neuron in the hidden layer can approximate any univariate function, *Neural Computation*, **28** (2016), 1289–1304.

[35] D. Costarelli, R. Spigler, Constructive Approximation by Superposition of Sigmoidal Functions, *Anal. Theory Appl.*, **29** (2013), 169–196.

[36] B. I. Yun, A Neural Network Approximation Based on a Parametric Sigmoidal Function, *Mathematics*, **7** (2019), 262.

[37] N. Kyurkchiev, Comments on the Yun's algebraic activation function. Some extensions in the trigonometric case, *Dynamic Systems and Applications*, **28**, No.3 (2019), 533–543.

[38] N. Kyurkchiev, A. Iliev, *Extension of Gompertz-type Equation in Modern Science: 240 Anniversary of the birth of B. Gompertz*, LAP LAMBERT Academic Publishing (2018), ISBN: 978-613-9-90569-0.

[39] S. Markov, N. Kyurkchiev, A. Iliev, A. Rahnev, On the approximation of the generalized cut functions of degree $p + 1$ by smooth hyper-log-logistic function, *Dynamic Systems and Applications*, **27**, No. 4 (2018), 715–728.

[40] A. Malinova, O. Rahneva, A. Golev, V. Kyurkchiev, Investigations on the Odd-Burr-III-Weibull cumulative sigmoid. Some applications, *Neural, Parallel, and Scientific Computations*, **27**, No. 1 (2019), 35–44.

[41] N. Kyurkchiev, A. Iliev, A. Rahnev, T. Terzieva, A new analysis of Code Red and Witty worms behavior, *Communications in Applied Analysis*, **23**, No. 2 (2019), 267–285.

[42] N. Kyurkchiev, A. Iliev, A. Rahnev, T. Terzieva, Some New Approaches for Modelling Large–Scale Worm Spreading on the Internet. II, *Neural, Parallel, and Scientific Computations*, **27**, No. 1 (2019), 23–34.

[43] N. Kyurkchiev, A. Iliev, A. Rahnev, T. Terzieva, A New Analysis of Cryptolocker Ransomware and Welchia Worm Propagation Behavior. Some Applications. III, *Communications in Applied Analysis*, **23**, No. 2 (2019), 359–382.

[44] N. Kyurkchiev, A. Iliev, A. Rahnev, A new class of activation functions based on the correcting amendments of Gompertz-Makeham type, *Dynamic Systems and Applications*, **28**, No. 2 (2019), 243–257.

[45] R. Anguelov, M. Borisov, A. Iliev, N. Kyurkchiev, S. Markov, On the chemical meaning of some growth models possessing Gompertzian-type property, *Math. Meth. Appl. Sci.*, (2017), 12 pp.

[46] N. Pavlov, A. Iliev, A. Rahnev, N. Kyurkchiev, *Some software reliability models: Approximation and modeling aspects*, LAP LAMBERT Academic Publishing, (2018), ISBN: 978-613-9-82805-0.

[47] N. Pavlov, A. Iliev, A. Rahnev, N. Kyurkchiev, *Nontrivial Models in Debugging Theory (Part 2)*, LAP LAMBERT Academic Publishing, (2018), ISBN: 978-613-9-87794-2.

[48] N. Kyurkchiev, A. Iliev, A. Rahnev, *Some Families of Sigmoid Functions: Applications to Growth Theory*, LAP LAMBERT Academic Publishing, (2019), ISBN: 978-613-9-45608-6.

[49] A. Iliev, N. Kyurkchiev, A. Rahnev, T. Terzieva, *Some models in the theory of computer viruses propagation*, LAP LAMBERT Academic Publishing, (2019), ISBN: 978-620-0-00826-8.

[50] S. Sarat, A. Terzis, HiNRG Technical Report: 01-10-2007 Measuring the Storm Worm Network, (2007).

[51] A. C. Crombie, On competition between different species of graminivorous insects, *Proceedings of the Royal Society B*, **132** (1945), 362–395.

[52] N. Radchenkova, M. Kambourova, S. Vassilev, R. Alt. S. Markov, On the mathematical modelling of EPS production by a thermophilic bacterium, *Biomath* **4**, (2014), 1–10.

[53] D. I. Wallace, X. Guo, Properties of tumor spheroid growth exhibited by simple mathematical models, *Front. Oncol.*, **3**, Art. No. 51 (2013), 9 pp.

[54] I. Hidrovo, J. Dey, M.E. Chesal, D. Shumilov, N. Bhusal, J. M. Mathis, Experimental method and statistical analysis to fit tumor growth model using SPECT/CT imaging: a preclinical study, *Quant. Imaging Med. Surg.*, **7**, No. 3 (2017), 299–309.

[55] G. Serazzi, S. Zanero, Computer Virus Propagation Models. In: Calzarossa M.C., Gelenbe E. (eds) Performance Tools and Applications to Networked Systems, MASCOTS 2003, *Lecture Notes in Computer Science*, **2965**, Springer, Berlin, Heidelberg (2004).

[56] D. Male, J. Brostoff, D. Roitt, *Immunology*, 8th ed., Elsevier, China (2012).

[57] S. Montero, R. Martin, A. Guerra, O. Casanella, G. Cocho, J. Nieto-Villar, Cancer Glycolysis I: Entropy Production and Sensitivity Analysis in Stationary State, *J. Adenocarcinoma*, **1**, No. 2 (2016), 7 pp.

[58] E. Lungu, T. J. Massaro, E. Ndelwa, N. Ainea, S. Chibaya, N. J. Malunguza, Mathematical modeling of the HIV/ Kaposi's sarcoma coinfection dynamics in areas of high HIV prevalence, *Comp. and Math. Meth. in Medicine*, **2013** (2013), 12 pp.

[59] M. Vinci, S. Gowan, F. Boxall, L. Patterson, M. Zimmermann, W. Court, C. Lomas, M. Mendiola, D. Hardisson, S. A Eccles, Advances in establishment and analysis of 3D tumor spheroid-based functional assays for target validation and drug evaluation, *BMC Biology*, **10**, No. 29 (2012), 51 pp.

[60] E. Bonyah, M. Khan, K. Okosun, J Gomez-Aguilar, On the co-infection of dengue fever and Zika virus, *Optim. Control Appl. Meth.*, (2019), 28 pp.

[61] J. Peters, *Foundations of Computer Vision: Computational Geometry, Visual Image Structures and Object Shape Detection*, Springer, Cham (2017).